Exploring the contribution of coal shrinkage to coal seam gas-induced subsidence

A research update paper

Version 1.0

April 2023

Document ID*: OGIA 23/M01*

Office of Groundwater Impact Assessment

Version	Release date	Authorised by
1.0	17 April 2023	Sanjeev Pandey

Overall guidance and direction: Gerhard Schöning and Sanjeev Pandey

Contributors: Hamid Aghighi, Gerhard Schöning, Tao Cui, Marti Burcet and Sanjeev Pandey

International peer review: A/Professor Nicolas Espinoza (University of Texas at Austin)

Acknowledgement: Dr Chris Leonardi and Professor Phil Hayes (University of Queensland) for highlighting the coal shrinkage process.

The work presented in this document provides an update on a component of OGIA's ongoing research to support the assessment and management of resource development impacts. It is not a statutory document. Conclusions are subject to further review and changes ahead of the preparation of the next Underground Water Impact Report and other statutory reporting as needed.

This research update paper should be referenced as:

Aghighi, H, Schöning, G, Cui, T, Burcet, M, Pandey, S, (2023). Exploring the contribution of coal shrinkage to coal seam gas induced subsidence: a research update paper by the Office of Groundwater Impact Assessment (OGIA), Department of Regional Development, Manufacturing and Water, Queensland Government. Australia. April 2023.

This publication has been compiled by the Office of Groundwater Impact Assessment, Department of Regional Development, Manufacturing and Water.

Table of contents

Table of figures

Table of tables

Abstract

Coal seam gas extraction involves two key subsurface processes: fluid flow primarily through coal fractures/cleats and gas desorption from the coal matrix. The former leads to the depressurisation of the coal seam and coal compaction, while the latter induces coal shrinkage. Both processes contribute to coal seam gas (CSG)-induced subsidence.

The amount of coal shrinkage in a given time period is proportional to the corresponding change in gas content. It also depends on coal properties, such as Langmuir isotherm and shrinkage strain parameters, which vary by coal composition and rank.

Past research has extensively addressed the effect of coal matrix shrinkage on coal permeability evolution through analysing measurements at both laboratory and field scales, as well as developing analytical and numerical models. Relatively little research, however, has been done on the effect of coal shrinkage on subsidence in CSG fields.

To explore the potential contribution of coal shrinkage to CSG-induced subsidence in the Surat Basin context, the Office of Groundwater Impact Assessment (OGIA) has developed, following the first principles, an analytical model for shrinkage strain, based on Langmuir-type relations between gas content and pore fluid pressure. This approach lends itself well to coupling with groundwater models, as the specific storage and pressure/head are the shared variables.

A bolt-on Monte Carlo uncertainty analysis shows that prior distributions of these parameters lend themselves to a range in shrinkage proportion of total subsidence (54-73% on average). These results suggest that coal shrinkage is likely to play an important role in the total subsidence realised at the surface. Prior distributions for the parameters result in a large range of uncertainty in the current analysis and further work to constrain these distributions can reduce predictive variability.

A subsequent sensitivity analysis on five key parameters for this model shows that the shrinkage proportion is sensitive to all five, however the top three relate to specific storages of interburden and coal and the Langmuir strain parameter.

Limited experimental data are currently available on the Langmuir strain and head parameters in the Surat Cumulative Management Area (Surat CMA). OGIA is exploring options to obtain measurements of Langmuir strain and head from core data in the Surat CMA to better constrain prior distributions for these parameters and to inform the development of predictive subsidence models.

OGIA's subsidence modelling presented in the Underground Water Impact Report 2021 is likely to have implicitly included the effect of coal shrinkage because of calibration against historical ground motion data. In future, more explicit representation of the process will allow further improvements to spatial and temporal resolution in predictions.

Glossary

The following key terms are used throughout this document and so a brief description is offered below:

Effective stress – stress applied to the grains of porous media, which is the total stress minus a fraction of the pore fluid pressure.

Poromechanical compaction – contraction of porous media due to increasing effective stress in response to pore fluid depressurisation.

Coal shrinkage – contraction of coal matrix due to gas desorption.

Total compaction – total combined reduction in thickness caused by both poromechanical compaction and coal shrinkage.

Subsidence – the component of ground movement that is induced by CSG depressurisation. This results from the total compaction in coal seams as well as of the interburden (the material between the individual coal seams) and the overburden (the strata above the coal seams).

Ground movement – also referred to as ‘ground motion’, the movement in ground surface elevation measured at surface, irrespective of the cause.

Nomenclature

c_m ..... uniaxial compressibility, $M^{-1}\ L^{1}\ T^{2}$

c_w..... water compressibility, $M^{-1}\ L^{1}\ T^{2}$

E ..... Young's modulus, $M^{1}\ L^{-1}\ T^{-2}$

G..... shear modulus, $M^{1}\ L^{-1}\ T^{-2}$

h ..... thickness, L^{1}

H..... hydrostatic head, L^{1}

H_f ..... hydrostatic head of the coal pore fluid, L^{1}

$H_{L\varepsilon}$ ..... Langmuir hydrostatic head, L^{1}

H_{fi}..... initial hydrostatic head of the coal pore fluid, L^{1}

H_{us} ..... uniaxial compaction modulus, $M^{1}\ L^{-1}\ T^{-2}$

i..... subscript for initial and an index denoting spatial coordinates

j..... an index denoting spatial coordinates *x*, *y* and *z*

K..... bulk modulus, $M^{1}\ L^{-1}\ T^{-2}$

k_{ep} ..... coefficient proportionality, $M^{-1}\ L^{1}\ T^{2}$

M ..... superscript for mechanical process

n ..... effective porosity, dimensionless

p_d ..... desorption pressure, $M^{1}\ L^{-1}\ T^{-2}$

p_f ..... fluid pressure, $M^{1}\ L^{-1}\ T^{-2}$

p_L ..... Langmuir pressure, $M^{1}\ L^{-1}\ T^{-2}$

$p_{L\varepsilon}$..... Langmuir pressure for shrinkage strain, $M^{1}\ L^{-1}\ T^{-2}$

S ..... superscript for sorption process

S_s ..... specific storage, L^{-1}

S_w ..... water saturation, dimensionless

t ..... time, T^{1} and a subscript for total

V_g ..... gas content, $M^{-1}\ L^{3}$

V_L ..... Langmuir volume, $M^{-1}\ L^{3}$

V_w ..... volume of produced water, L^{3}

V_{wr} ..... volume of produced water due to rock compaction, L^{3}

V_{wp} ..... volume of produced water due to water expansion, L^{3}

V_{wp} ..... volume of produced water due to coal shrinkage, L^{3}

V_{pv} ..... pore volume contraction, L^{3}

V_T ..... rock volume, L^{3}

Greek symbols

α_b..... Biot's coefficient, dimensionless

β_h..... Langmuir strain to Langmuir volume, dimensionless

γ_w..... specific weight of water, $M^1 L^{-2} T^{-2}$

ε ..... strain, dimensionless

ε_b ..... bulk strain, dimensionless

λ ..... first Lame's constant, $M^1 L^{-1} T^{-2}$

σ ..... stress, $M^1 L^{-1} T^{-2}$

σ' ..... effective stress, $M^1 L^{-1} T^{-2}$

σ_m ..... mean stress, $M^1 L^{-1} T^{-2}$

ν ..... Poisson's ratio, dimensionless

1 Introduction

1.1 Primary target audience

This document is primarily targeted to a scientific audience. Fundamental understanding of geological and geomechanical principles, and coal seam gas (CSG) production processes is implied.

1.2 Context

The Office of Groundwater Impact Assessment (OGIA) included a regional assessment of CSG-induced subsidence in the Surat CMA in the Underground Water Impact Report (UWIR) 2021 (OGIA 2021). This included both monitoring and modelling of CSG-induced subsidence. The subsidence modelling adopted by OGIA for the UWIR was built on its latest regional groundwater model – a highly parameterised pseudo-dual-phase numerical groundwater model, constrained by a stochastic calibration with a multi-component objective function. After extensive testing, comparison and validation with numerical subsidence models, an analytical poromechanical compaction calculation was developed and integrated with the regional groundwater model. Interferometric Synthetic Aperture Radar (InSAR) observations were subsequently used, in conjunction with rejection sampling of stochastic parameter fields, to facilitate a predictive uncertainty analysis of subsidence in the Surat CMA (OGIA 2021).

As an ongoing improvement, OGIA continues to research the processes affecting CSG-induced subsidence, collecting and integrating additional data to improve the groundwater flow and subsidence modelling.

In recent times, a particular focus for researchers outside OGIA has been on the potential contribution to CSG-induced subsidence of desorption-induced shrinkage processes of coal seams, alongside poromechanical compaction (Liu et al. 2021; T. Liu et al. 2022; Yang & Luo 2021; Hummel et al. 2021). In particular, the University of Queensland has recently been actively exploring this aspect. Prompted by those works, OGIA also commenced exploring the potential contribution of desorption-induced shrinkage to the total CSG-induced subsidence in the context of Surat Basin where it is overlain by the Condamine Alluvium. Findings from this work will inform further development and enhancement of OGIA subsidence models.

It is to be noted, however, that OGIA's subsidence modelling presented in the UWIR 2021 is likely to have implicitly included the effect of coal shrinkage. In future, more explicit representation of the process will allow further improvements to spatial and temporal resolution of predictions.

1.3 Scope

This document provides an update on OGIA's research into the potential contribution of coal shrinkage to overall CSG-induced subsidence, and how it may affect assessment of subsidence in the Surat Basin. Specifically, it covers the following aspects:

- a review of processes relevant to coal shrinkage and how they have been considered so far
- a theoretical basis for coal shrinkage and its relationship with hydrogeological processes and poromechanical compaction
- a stochastic analysis to explore the relative contribution of coal shrinkage to overall subsidence in the context of the Surat Basin

- traditional sensitivity analysis to explore the contribution of key parameters affecting the potential contribution of coal shrinkage to subsidence
- commentary on ongoing work in this space and how it may contribute to the modelling of subsidence and groundwater flow in the future.

Due to the continual evolution of knowledge and the progressive nature of research, the findings presented herein will be continually reviewed and updated in subsequent research updates where necessary.

1.4 Linkages to OGIA's overall subsidence research program

The work presented here is part of a larger and ongoing research program to assist the development of OGIA's subsidence assessment and to inform predictive groundwater modelling in the Surat CMA.

This work forms part of a project to develop locally integrated subsidence models, subject to ongoing considerations of OGIA's wider scope of work in this space. It provides the theoretical basis for an analytical model (accounting for shrinkage effects) which can be integrated with numerical groundwater models. These models will be designed to leverage large observational datasets from InSAR and will be coupled with various signal models through a signal separation process to obtain high resolution maps of historical CSG-induced subsidence.

The predictive impact assessment will also draw heavily on LiDAR data to derive a baseline surface against which to assess changes.

Linkages between various pieces of work in this context are presented in Figure 1 below.

It is expected that further research update papers on these various components will be published as the research program progresses.

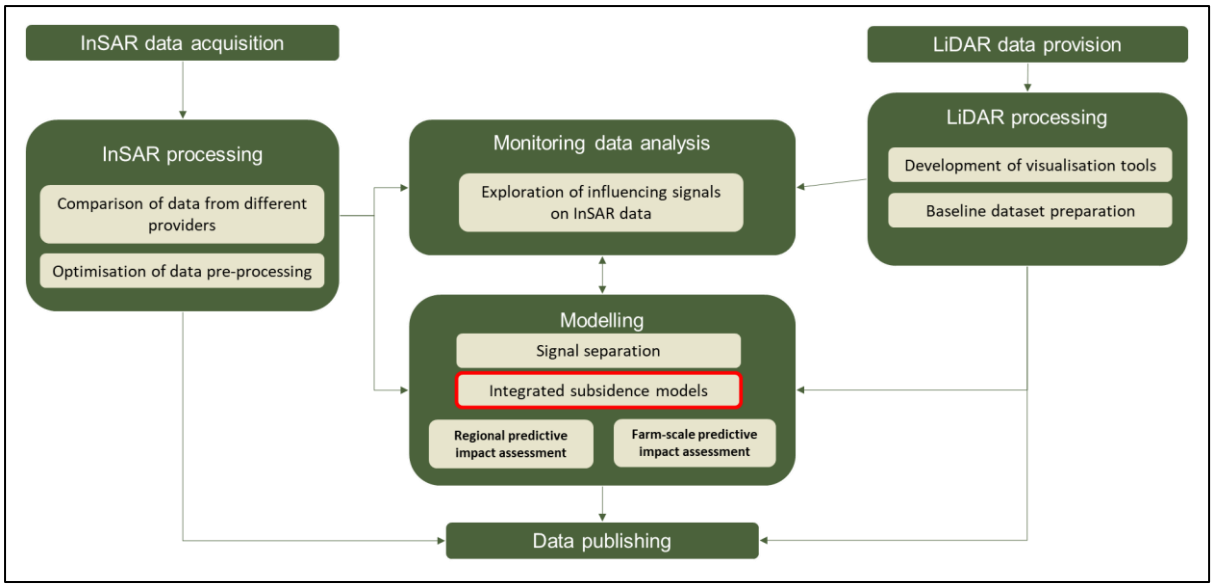

Figure 1: A schematic representation of OGIA's research program for the assessment of subsidence and groundwater modelling

2 Background

2.1 The subsidence process and coal shrinkage

Coal seams are fractured heterogenous media comprising macropores and micropores and fractures varying in size from a few angstroms to more than a micrometre. Macropores are typically the cleats that are developed as two different sets (i.e. face and butt cleats) perpendicular to each other, while micropores are within the matrix that is separated by those cleats (Figure 2).

Micropores in the matrix provide storage of hydrocarbons (mostly in the form of gas) and water, while macropores facilitate flow – similar to a dual-porosity flow system, where gas is present in a free state and flows under Darcy flow principles (e.g., Cui & Bustin 2005).

CSG production involves subsurface physical processes such as diffusion, fluid flow and geomechanics (Aghighi, Lv & Roshan 2021; Espinoza et al. 2013; Wei & Zhang 2010; Wu et al. 2010). Diffusion governs gas desorption from the coal matrix into coal cleats. The gas content gradient between the matrix and cleats drives this transport process and is governed by diffusivity – a key coal property. Darcy flow takes place within the cleats where fluid leaked from the matrix moves towards the borehole under the prevalent pressure gradient. This flow is a function of both coal and fluid properties such as effective permeability, porosity and fluid saturation. The third process is geomechanical, which governs coal deformation.

Extracting water and gas from coal seams – as part of CSG operations – can lead to compaction within the coal seams, the interburden and the overburden material. This subsurface compaction is then manifested as subsidence at the ground surface. The amount of subsidence at the surface increases with pressure decline (caused by fluid withdrawal), rock compressibility and reservoir thickness.

In terms of processes, the total compaction in the coal seams – i.e. combined reduction in thickness – is caused by two distinct processes: poromechanical compaction and coal shrinkage. Poromechanical compaction is the compaction resulting from a decrease in porous space – primarily the coal cleats. Concurrent to this, gas desorption from the coal matrix also leads to the contraction of coal, which is referred to as shrinkage. It is to be noted that shrinkage is unique to sorptive rocks (i.e. coal herein), whereas compaction can occur in all porous rocks, including coal. These two mechanisms are the major sources of subsidence induced by the extraction of subsurface fluid (Holzer & Galloway 2005; Galloway & Burbey 2011).

Numerous studies and field observations have shown that subsidence can occur in response to the extraction of subsurface fluids (e.g. water, oil and gas) from aquifers and conventional reservoirs (Poland & Davis 1969; Khan, Huang & Karacay 2014; Morton, Bernier & Barras 2006; Teatini et al. 2006). This issue has also been studied in relation to CSG fields, although to a far lesser extent (Meredith et al. 2015; Jayeoba 2020; Naraj 2020; Commonwealth of Australia 2014). The contribution of coal shrinkage to subsidence, however, has received little attention worldwide, despite extensive investigation of the coal shrinkage effect on permeability evolution (Chen et al. 2013; Cai et al. 2014; Lv, Cheng, et al. 2021; Shi & Durucan 2004; Cui & Bustin 2005; Palmer & Mansoori 1998; Pan & Connell 2012) and wellbore stability (J. Liu et al. 2022; Karthikeyan, Chand & Chatterjee 2020).

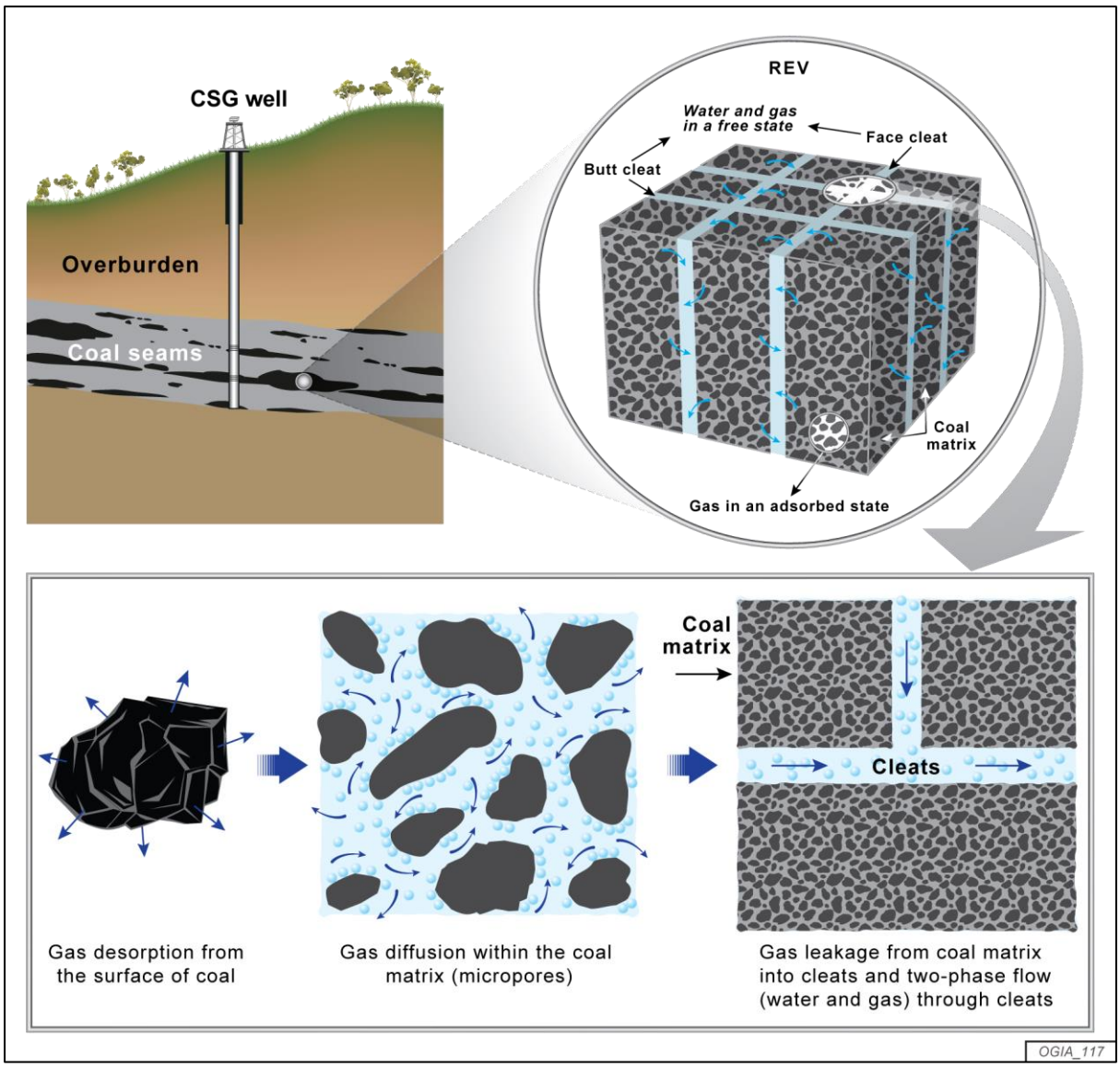

Figure 2: Coal consists of matrix and cleats where the dominant fluid transport processes are diffusion and Darcy flow, respectively (modified from (Schlumberger n.d.))

2.2 Coal shrinkage in reservoir engineering

Coal shrinkage has recently been studied in the context of reservoir engineering. Past research introduced numerous relations for the effect of coal shrinkage on coal permeability. Pan and Connell (2012) presented an extensive review on permeability evolution in coal. It is well known that in aquifers and conventional reservoirs, pore pressure depletion tends to reduce permeability and hence productivity. This effect is more pronounced in naturally fractured tight formations where depressurisation leads to the closure of fractures as main conduits for fluid flow. Given the proportionality of permeability to the cube of fracture aperture as per the cubic law, a small decrease in fracture aperture of a formation, caused by depressurisation, results in a relatively significant reduction in the effective permeability of the formation. The shrinkage process – which is unique to sorptive rocks – makes coal permeability evolution more complex.

Change to coal fracture aperture is affected by both depressurisation and shrinkage. Gas pressure drops lead to an increase in effective stress acting on fracture planes (hydro-mechanical effect) thus closing fractures, whereas desorption-induced shrinkage (sorptive-mechanical effect) tends to open

coal fractures. The prevailing mechanism between these two indicates the overall change in the aperture and hence fracture permeability during drainage (Aghighi et al. 2022). Analytical and numerical models have shown that the prevailing mechanism may switch, in both time and space (Burgoyne & Shrivastava 2016; Pan & Connell 2012). In other words, the permeability of a sorptive gas-bearing formation may initially drop (due to the prevalence of hydro-mechanical effect) and then rebound as the effect of matrix shrinkage prevails. In some sedimentary basins around the world, unexpected rises in gas production after periods of decline have been attributed to this phenomenon (Palmer & Mansoori 1996; Aghighi, Lv & Roshan 2021).

Existing permeability models accounting for coal shrinkage range from sophisticated numerical models to simplified analytical models. See Pan & Connell (2012) for an extensive review on coal permeability models. Sophisticated numerical models incorporate more contributing processes in a coupled manner, at the cost of extensive computational resources and time for most field applications (Wu et al. 2010; Aghighi, Lv & Roshan 2021; Wei & Zhang 2010). Analytical or semi-analytical coal shrinkage models compromise some degrees of accuracy to improve practicality. These models, if coupled with calibrated fluid flow models, can facilitate significant benefits when coupled with a rigorous uncertainty analysis and so may be well suited for field applications.

2.3 Potential for shrinkage-induced subsidence in the Surat Basin

Coal shrinkage caused by extracting gas from tens of metres of coal in the Surat Basin has the potential to affect subsidence at the ground surface. This is in addition to poromechanical compaction of coal seams, which results from the depressurisation induced by water and gas extraction from coal. The magnitude depends on the coal thickness, the shrinkage properties, the drawdown, the depth of coal seams and the competence of overlying formations. These factors can vary spatially depending on the stratigraphy, structural features and geological characteristics of coal and non-coal formations, including rock mechanical properties, as well as coal rankings and types.

In the Surat and Bowen Basins, coal shrinkage has been the subject of research in the area of coal permeability evolution (Salmachi et al. 2021; Raza et al. 2020; Bottomley et al. 2017) and wellbore stability (Zhong et al. 2021; Reisabadi et al. 2020). Limited research has been undertaken to date in relation to subsidence (Masoudian et al. 2019; Commonwealth of Australia 2014). However, as mentioned previously, the University of Queensland is currently conducting research to explore coal shrinkage in the context of subsidence.

InSAR and LiDAR measurements of the ground surface movement, in conjunction with numerical modelling, have shown that subsidence can occur as a result of CSG extraction (OGIA 2021), however the contribution of different processes in the total subsidence is not separated. Masoudian et al. (2019) constructed a numerical model for the simulation of the ground surface movement that incorporated the coal shrinkage process, together with poromechanical compaction due to depressurisation. They concluded that their numerical subsidence results are affected by coal shrinkage.

3 Fundamental principles and concepts

Methods both numerical and analytical are employed to assess geomechanical processes. Numerical models can incorporate more interacting processes with fewer assumptions, thereby providing more refined results; however, they need relatively extensive computational resources and time, limiting opportunities for calibration and uncertainty quantification.

In comparison, analytical or semi-analytical models compromise some degrees of accuracy to improve computational efficiency and allow greater flexibility for data-driven models that are less reliant on processes. Analytical models are widely used for the estimation of subsidence induced by subsurface fluid production (Zoback 2010; Erling Fjær, Rune Holt, Per Horsrud 2008). They lend themselves well to coupling with groundwater models – similar to the one developed by OGIA – as the pressure/head is the shared variable.

In this context, this chapter discusses fundamental concepts and principles underpinning analytical modelling of poromechanical compaction. Extended models are then presented to include the effect of desorption-induced shrinkage in sorptive rocks such as coal on subsidence.

3.1 Gas adsorption and desorption

The gas adsorption capacity of coal seams follows the Langmuir theory of adsorption whereby the maximum amount of gas that coal seams can store depends on their fluid pressure and temperature. Based on the Langmuir isotherm (constant temperature), the capacity of coal seams for holding gas increases non-linearly with their pore fluid pressure (Figure 3a).

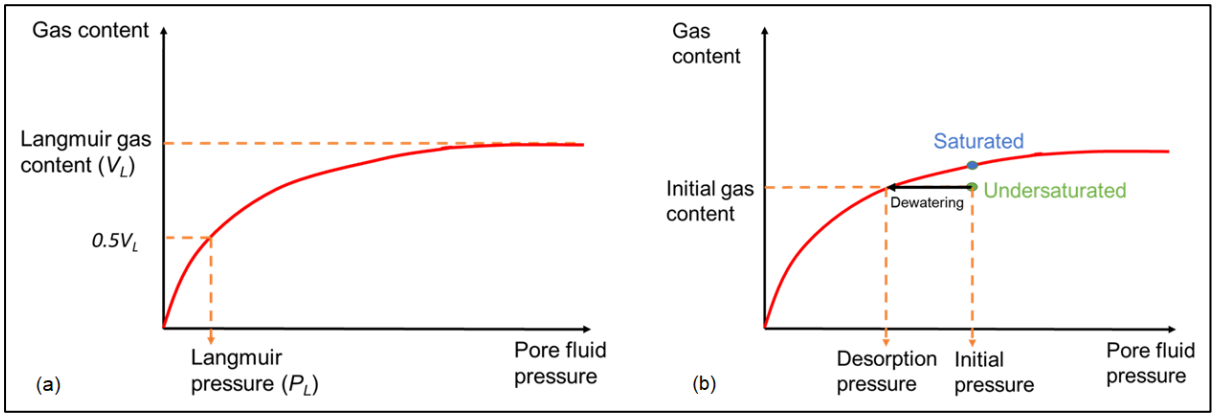

Figure 3: a) adsorption/desorption Langmuir isotherm curve and b) saturated and undersaturated coal

The Langmuir isotherm curve can be described by Eq (1):

$$V_g = V_L \frac{p_f}{p_L + p_f} \quad (1)$$

where V_g is the gas content, p_f is the pore fluid pressure, and V_L and p_L are the Langmuir volume and pressure, respectively (Gray 1987).

Imposing a gas content (concentration) gradient to the coal matrix drives a diffusion process that tends to establish an equilibrium state across the coal domain (consisting of the matrix and cleats).

This is a transient process in general; however, assuming a pseudo-steady non-equilibrium gas desorption based on Fick's first law, the rate of diffusion can be given by (Wei & Zhang 2010):

$$-\frac{\partial V_g}{\partial t} = \frac{\Delta V_g}{\tau} \quad (2)$$

where V_g is the gas content in pores, ΔV_g is the gas content differential between cleats and micropores, t is time and τ is the sorption time – a lumped parameter controlling the rate at which the adsorbed gas is released (i.e. desorbed from and diffused through) micropores into the cleats. Sorption time data are routinely measured as part of gas desorption analysis of core samples in laboratories and reported.

Depending on whether the gas content of coal is equal or below its maximum gas storage capacity at the current (initial) pore fluid pressure, coal seams can be in either a saturated or an undersaturated state. Where undersaturated, gas desorption (hence production) will not take place unless pore fluid pressure falls below a certain pressure, called desorption pressure (Figure 3b). The depressurisation of coal seams typically requires initial dewatering, through pumping. Once the desorption pressure is reached, the desorbed gas starts diffusing into coal cleats and then flows towards the wellbore.

3.2 Poromechanical compaction

Typical oil and gas reservoirs have large lateral extents relative to their thicknesses. As a result, their production-induced compaction is predominantly vertical rather than lateral. Analytical models based on the uniaxial compaction approach are therefore often used for the estimation of compaction in such reservoirs. These models are based on following simplifying assumptions (Zoback 2010):

- The reservoir is homogeneous and behaves as a linear elastic medium (within the applied load range).
- The process is isothermal.
- The reservoir has a large lateral extent relative to its thickness.
- Compaction only takes place along the vertical direction (i.e. lateral displacements are negligible).
- Total vertical in-situ stresses (in terms of both magnitude and direction) are not influenced by fluid extraction.

Hooke's law for linear elastic material is expressed as follows:

$$\varepsilon_{xx} = \frac{1}{E}\left[\Delta\sigma'_{xx} - \nu\left(\Delta\sigma'_{zz} + \Delta\sigma'_{yy}\right)\right] \quad (3)$$

$$\varepsilon_{yy} = \frac{1}{E}\left[\Delta\sigma'_{yy} - \nu(\Delta\sigma'_{zz} + \Delta\sigma'_{xx})\right] \quad (4)$$

$$\varepsilon_{zz} = \frac{1}{E}\left[\Delta\sigma'_{zz} - \nu\left(\Delta\sigma'_{xx} + \Delta\sigma'_{yy}\right)\right] \quad (5)$$

where E and ν are the drained Young's modulus and Poisson's ratio of the bulk material, respectively, ε is the strain, σ is the stress, the prime symbol (´) indicates the effective stress and Δ denotes changes with respect to the reference situation. Subscripts x, y and z refer to the mutually orthogonal coordinates assumed to be along the principal orientations of in-situ stresses (z being vertical).

Applying the assumption of negligible lateral strains ($\varepsilon_{xx} = \varepsilon_{yy} = 0$) on the Hooke's law leads to:

$$\Delta\sigma'_{xx} = \Delta\sigma'_{yy} = \frac{\nu}{1-\nu}\Delta\sigma'_{zz} \quad (6)$$

If there is no formation-shielding or stress-arching, the total vertical stress will be constant ($\Delta\sigma_{zz} = 0$). The vertical effective stress then becomes:

$$\Delta\sigma'_{zz} = -\alpha_b \Delta p_f \tag{7}$$

where p_f is the fluid pressure and α_b is the Biot's coefficient.

Substituting Eq (6) and Eq (7) into Eq (5) gives:

$$\varepsilon_{zz} = -\frac{\alpha_b \Delta p_f}{\frac{E(1-\nu)}{(1+\nu)(1-2\nu)}} \tag{8}$$

and replacing $\varepsilon_{zz} = -\frac{\Delta h}{h}$ (note the adopted sign convention) gives:

$$\Delta h = \frac{\alpha_b}{\frac{E(1-\nu)}{(1+\nu)(1-2\nu)}} h \Delta p_f \tag{9}$$

or:

$$\Delta h = \alpha_b c_m h \Delta p_f \tag{10}$$

where $c_m$is the compaction coefficient or uniaxial compressibility. This coefficient is the inverse of uniaxial compaction modulus H_{us} (also referred to as oedometer modulus $H_{us} = (d\sigma_{zz})/(d\varepsilon_{zz})$), which is one of the elastic moduli (Erling Fjær, Rune Holt, Per Horsrud 2008):

$$c_m = \frac{1}{H_{us}} = \frac{1}{\lambda + 2G} \tag{11}$$

where λ is the first Lame's constant and G is the shear modulus of the rock (equals the second Lame's constant μ).

3.3 Coal shrinkage

Laboratory experiments show that gas desorption from sorptive rocks such as coal results in the shrinkage of the rocks' solid constituent (Lv, Aghighi, et al. 2021; Durucan, Ahsanb & Shia 2009) – referred to as matrix shrinkage. From a geomechanical perspective, the ratio of coal volumetric shrinkage to the reference volume is called the shrinkage strain (denoted by ε^S). Existing empirical models for ε^S relate it to the reduction in either pore fluid pressure or gas content.

The simplest form of such models assumes a linear relationship between the shrinkage strain and pore fluid pressure (Gray 1987):

$$\Delta\varepsilon^S = k_{ep} \Delta p_f \tag{12}$$

where $k_{ep}$is the coefficient of proportionality.

Levine (1996) showed that a linear relationship overestimates the shrinkage strain and presented a Langmuir-type relationship as follows (Figure 4a):

$$\varepsilon^S = \varepsilon_L \frac{p_f}{p_{L\varepsilon} + p_f} \tag{13}$$

where $\varepsilon_L$is the maximum sorption-induced volumetric strain under infinite pore fluid pressure (hereafter Langmuir strain) and $p_{L\varepsilon}$ is the Langmuir pressure for sorption-induced strain, which is the pressure corresponding to half of ε_L. It is worth noting the difference between the Langmuir pressure in the context of gas content capacity versus pressure (i.e., p_L in Eq (1)) and in relation to changes in sorption strain versus pressure (i.e., $p_{L\varepsilon}$ in Eq (13)).

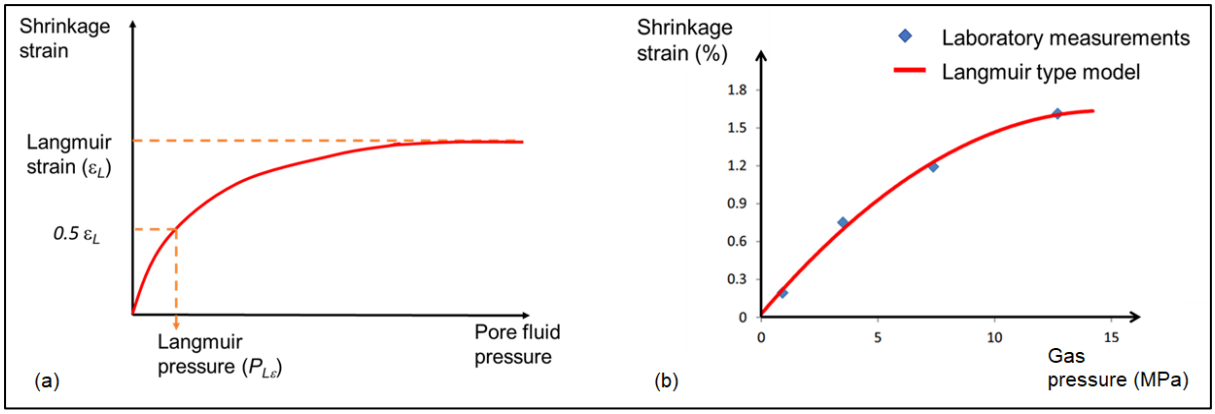

Figure 4: a) Langmuir-type curve representing shrinkage strain as a function of pore fluid pressure; b) curve-fitting of laboratory experiment results to obtain Langmuir parameters

The Langmuir-type relation has been widely used in characterising sorption strain (Harpalani & Schraufnagel 1990; Robertson & Christiansen 2006; Wu et al. 2010; Palmer & Mansoori 1998). Langmuir strain parameters are in fact curve-fitting parameters obtained from laboratory experiments of coal shrinkage under different pore fluid pressures for a coal sample (Figure 4b). It is noted that these parameters are commonly obtained from adsorption/swelling experiments and their use for desorption/shrinkage processes is subject to the assumption of reversibility of sorption processes.

The Langmuir volumetric strain (ε_L) can have a linear relationship with Langmuir volume (Harpalani & Chen 1992):

$$\varepsilon_L = \beta_h V_L \tag{14}$$

where β_h is the ratio of Langmuir strain to Langmuir volume. In the absence of experimental data for shrinkage strain, Eq (14) can be used to estimate the Langmuir strain parameters provided β_h and V_L data are available or can be estimated (Robertson 2005).

The Langmuir strain (ε_L) can be measured under different boundary conditions, hence it can be a volumetric or a uniaxial value (e.g. using pressure or triaxial cells, respectively). Since the uniaxial strain is a widely accepted loading for subsidence, the Langmuir strain to be used in subsidence modelling should be consistent. If the Langmuir strain is available as a volumetric value – which is often the case – then its uniaxial equivalent should be evaluated for subsidence modelling.

Following Eq (14), the change in the sorption-induced volumetric strain during CSG depressurisation (Shi & Durucan 2004; Palmer & Mansoori 1998) is given by (note the compression-positive sign convention):

$$\Delta\varepsilon^S = \varepsilon^S - \varepsilon_i^S = -\varepsilon_L\left(\frac{p_f}{p_{L\varepsilon} + p_f} - \frac{p_{fi}}{p_{L\varepsilon} + p_{fi}}\right) \tag{15}$$

Where $p_{fi}$is the initial pressure corresponding to the reference state. Eq (15) assumes that the current and initial pressures are both below the desorption pressure. The implication of desorption pressure for the calculation of $\Delta\varepsilon^S$ is discussed subsequently. It is noted that shrinkage strain increases as pressure reduces, i.e. $\Delta\varepsilon^S > 0$ (note the sign convention of compression being positive in this article). In other words, since $p_{fi} > p_f$ (as production implies), thus $\varepsilon_i^S < \varepsilon^S$.

Eq (15) returns a shrinkage strain difference corresponding to a change in pore fluid pressure relative to an initial state. As outlined earlier, it takes time for the coal domain to reach an equilibrium state because of the diffusion process in the coal matrix. This is referred to as the sorption time, which is

influenced by the fluid type, cleat geometry, and diffusivity of the coal matrix. OGIA is currently assessing different approaches for considering the effect of sorption time in Eq (15), which allows a more realistic representation of the gas desorption and matrix shrinkage process.

3.3.1 Saturation state of coal

Evaluating shrinkage strain in coal seams requires the knowledge of their saturation states and desorption pressures. As Figure 5 shows, coal is at a saturated state if its gas content equals the corresponding gas capacity for a given pore pressure (based on its Langmuir isotherm curve). Similarly, coal is undersaturated if the gas content is lower than the corresponding gas capacity for a given pore pressure. The gas desorption pressure is the pore pressure at which gas desorption, and hence shrinkage in coal seams, starts. Dewatering from coal seams is thus required to reduce pore pressure in undersaturated coal below the gas desorption pressure.

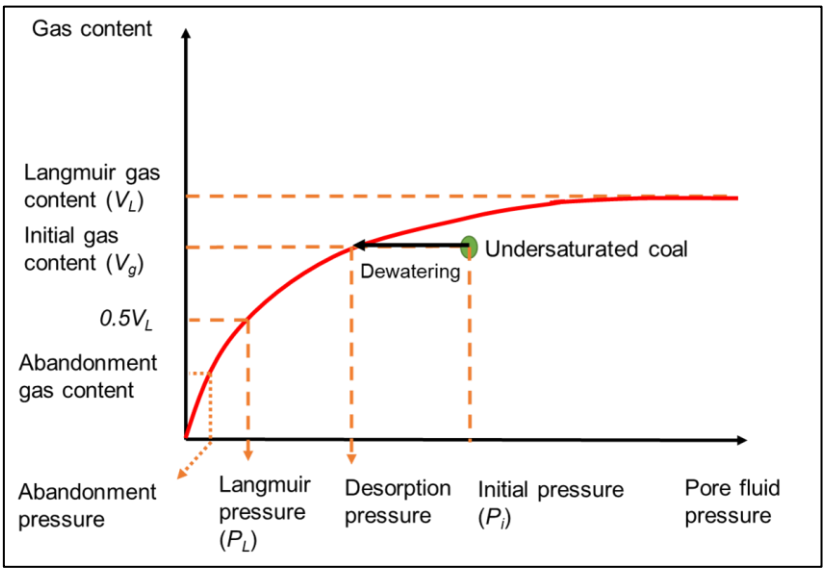

Figure 5: Gas sorption isotherm and the saturation state of coal

To calculate the change in shrinkage strain using Eq (15), pore pressures need to be checked against the desorption pressure to determine the corresponding state of coal in terms of saturation and the appropriate pressure to use for the calculation of initial and current shrinkage strains:

- if $p_{fi} < p_d$ then $\varepsilon_i^S = \frac{\varepsilon_L p_{fi}}{p_{L\varepsilon}+p_{fi}}$ otherwise $\varepsilon_i^S = \frac{\varepsilon_L p_d}{p_{L\varepsilon}+p_d}$
- if $p_f < p_d$ then $\varepsilon^S = \frac{\varepsilon_L p_f}{p_{L\varepsilon}+p_f}$ otherwise $\varepsilon^S = \frac{\varepsilon_L p_d}{p_{L\varepsilon}+p_d}$

where p_d is the desorption pressure.

3.3.2 Estimating desorption pressure from core data

Gas content and Langmuir isotherm data can be used to estimate the gas desorption pressure. These data are obtained from gas desorption and methane adsorption isotherm reports for cored boreholes. The general procedure entails the following:

- estimating the initial gas content from a gas content–depth empirical relation (e.g. a polynomial relation, $V_g = a\,(Depth - b)^c$) and
- estimating the desorption pressure from the corresponding Langmuir Isotherm equation.

Gas content–depth empirical relations can be obtained through a curve-fitting practice for each coal layer from available gas desorption reports in the area of interest, as shown in Figure 6 for samples in the Surat Basin (Queensland Government, Department of Resources, 2016). It is noted that a meaningful correlation may not always exist between gas content data and depth. The Langmuir isotherm parameters are also obtained from methane adsorption reports. These parameters are measured in the laboratory for different samples representing a certain interval in the coal measure. It is noted that gas content and Langmuir isotherm parameters vary with ash and moisture. The dry-ash-free (DAF) values should therefore be corrected for ash and moisture.

In the subsequent analysis, it is assumed that the initial pressure is less than the desorption pressure and thus shrinkage will occur immediately after depressurisation. This leads to a conservative (overestimating) assessment of coal shrinkage.

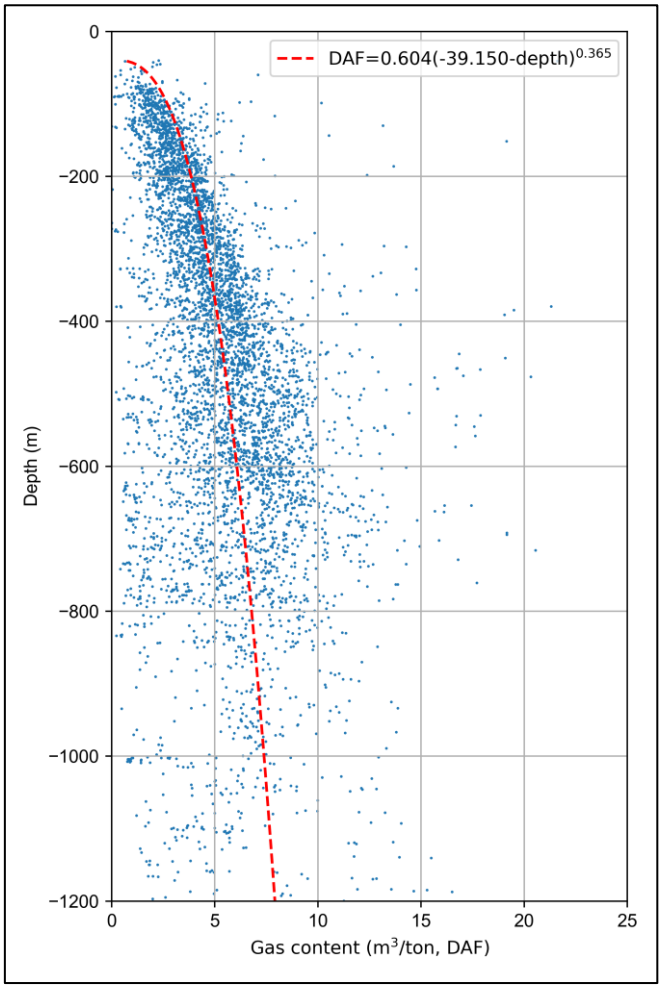

Figure 6: Gas content versus depth from 216 petroleum exploration wells in the Surat Basin

3.4 Total compaction

This section presents the derivation of total compaction of coal seams in response to CSG production. As aforementioned, gas extraction results in poromechanical compaction and shrinkage of coal seams (Harpalani & Schraufnagel 1990). Poromechanical compaction has been long known and studied as the source of subsidence induced by groundwater extraction from aquifers (Hanson, Anderson & Pool 1990; Holzer & Galloway 2005) and by petroleum production from conventional oil

and gas reservoirs (Nagel 2001; Geertsma 1973). Limited research, however, has paid attention to the effect of coal shrinkage on subsidence.

Desorption-induced shrinkage and thermal contraction are widely considered to be analogous processes when coupled with elastic deformation (Bear & Corapcioglu 1981; Cui & Bustin 2005; Palmer & Mansoori 1998; Shi & Durucan 2004). In thermoelasticity, the assumption of linearity implies that the total strain is the sum of mechanical and thermal strains where the medium is under both external loading and temperature changes (Jaeger, Cook & Zimmerman 2007). This implies the following in the context of coal shrinkage (Pan & Connell 2012):

$$d\varepsilon = d\varepsilon^M + d\varepsilon^S \tag{16}$$

where d denotes increment, ε is the strain and superscripts *M* and S refer to the mechanical and sorption processes, respectively. It is noted that Eq (16) holds under different loadings, such as hydrostatic or uniaxial strain (oedometeric). The stress-strain relationship for a homogeneous, isotropic, thermoelastic porous medium can be written as:

$$\Delta\sigma_{ij} = 2G\Delta\varepsilon_{ij} + \lambda\Delta\varepsilon\delta_{ij} + 3K\alpha_T\Delta T\delta_{ij} \tag{17}$$

where α_T is the coefficient of linear thermal expansion, ε is the volumetric strain, δ_{ij} is the Kronecker delta, *T* is the temperature and K is the bulk modulus ($K = \lambda + \frac{2}{3}G$).

A direct analogy between thermal contraction and matrix shrinkage leads to the stress-strain relationship for an isothermal sorptive coal seam as follows:

$$\Delta\sigma_{ij} = 2G\Delta\varepsilon_{ij} + \lambda\Delta\varepsilon\delta_{ij} + K\Delta\varepsilon^S\delta_{ij} \tag{18}$$

Following similar derivation for the poromechanical compaction in uniaxial strain conditions (section 3.2) and using Eq (15), the total compaction can be derived as follows:

$$\Delta h = c_m h\alpha_b\Delta p_f + h\varepsilon_L\frac{K}{H_{us}}\left(\frac{p_f}{p_{L\varepsilon} + p_f} - \frac{p_{fi}}{p_{L\varepsilon} + p_{fi}}\right) \tag{19}$$

where *K* is the bulk modulus of coal. It is noted that Eq (19) returns a negative value for production (depressurisation), reflecting a reduction in thickness. While Eq (19) accounts for the rock deformation processes associated with the withdrawal of water and gas from coal seams, it is desirable to link it to fluid flow, which is another major contributing process. Specific storage is a parameter that can link the two processes (chapter 4).

3.5 Subsidence

Based on previous work undertaken in the Surat CMA by OGIA (2021), the subsidence realised at the surface can be approximated by the cumulative settlement of underlying individual geological units. It can be expressed in a mathematical form as:

$$\Delta h_t = \sum_{i=1}^{m}\Delta h_i = -\sum_{i=1}^{m}(\varepsilon_{zz})_i h_i \tag{20}$$

where Δh is the vertical displacement, ε_{zz} is the vertical strain, h is the formation thickness, *m* is the number of formations, subscript *t* denotes total and i is the iteration index. Geomechanics sign convention is adopted here, which considers compression as positive. Fluid pressure and compressive stresses and strains are therefore considered positive. Eq (20) implies the assumption of no shielding (or bridging) effects.

The vertical strain (ε_{zz}) of each formation is determined from the knowledge of mechanical (e.g. elastic, elastoplastic, plastic, viscoelastic) behaviour, rock properties, loads, pressures, loading paths and boundary conditions. Different approaches have been used for the evaluation of subsidence induced by fluid withdrawal from non-sorptive rocks. These approaches may differ in terms of dimensions (2D versus 3D), mechanical (e.g. anisotropic, monoclinic, orthotropic, transversely isotropic) properties, mechanical behaviour, boundary conditions (plain strain/stress, 3D stress and pressure fields) and so on. Uniaxial strain/compaction is the most widely used approach, in terms of loading and boundary condition, for the evaluation of depressurisation-induced compaction (Erling Fjær, Rune Holt, Per Horsrud 2008; Zoback 2010; Dudley et al. 2016).

4 Linking poromechanical and hydrogeological parameters

As described in chapter 1, the subsidence model forms a part of the integrated modelling framework to assess potential CSG-related subsidence impact. CSG-induced subsidence is primarily influenced by poromechanical and hydrogeological processes. One of the aquifer parameters that is involved in the OGIA's groundwater model is specific storage. This is a poroelastic parameter that accounts for aquifer compaction and effective porosity, thus it has the capacity to link the two processes affecting subsidence – fluid flow and geomechanics. This chapter introduces this property in the context of groundwater modelling, although the definition can be extended to other reservoir rocks (Freeze & Cherry 1979; Jaeger, Cook & Zimmerman 2007; Erling Fjær, Rune Holt, Per Horsrud 2008).

4.1 The compaction coefficient and specific storage

The specific storage of an aquifer under uniaxial deformation is defined as the volume of water that a unit volume of rock produces under a unit reduction in hydraulic head. The volume of produced water is given by (Freeze & Cherry 1979):

$$dV_w = dV_{wr} + dV_{wp} \tag{21}$$

where dV_w is the total volume of produced water, dV_{wr} is the volume of produced water due to rock compression and dV_{wp} is the volume of produced water due to the expansion resulting from pressure decline.

The volume of produced water due to rock compression (dV_{wr}) is equal to pore volume contraction (dV_{pv}) caused by hydraulic head decline. If the change in the bulk volume of rock is assumed to be equal to the change in pore volume (i.e., the Biot's coefficient is equal one), the bulk strain (ε_b) due to an increase in the effective mean stress (σ'_m) can be expressed as:

$$d\varepsilon_b = \frac{dV_{wr}}{V_T} = \frac{dV_{pv}}{V_T} = c_m d\sigma'_m \tag{22}$$

The effective mean stress is given by:

$$\sigma'_m = \frac{1}{3}\left(\sigma'_{xx} + \sigma'_{yy} + \sigma'_{zz}\right) = \sigma_m - \alpha_b p_f \tag{23}$$

where σ_m is the total mean stress. Thus:

$$d\sigma'_m = d\sigma_m - \alpha_b dp_f \tag{24}$$

with negligible shielding and total stresses changes (due to change in pore pressure) leads to $d\sigma_m = 0$, thus:

$$d\sigma'_m = -\alpha_b dp_f \tag{25}$$

Combining Eq (22) and Eq (25) gives:

$$d\varepsilon_b = -c_m \alpha_b dp_f \tag{26}$$

With $dp_f = \gamma_w dh$, Eq (26) becomes:

$$d\varepsilon_b = -c_m \alpha_b \gamma_w dh \tag{27}$$

where γ_w is the specific weight of water ($\gamma_w = \rho g$), ρ is the water density, g is the acceleration due to gravity. Thus:

$$dV_{wr} = -V_T c_m \alpha_b \gamma_w dh \tag{28}$$

From this equation, we can obtain the volume of water produced by a unit volume of rock ($V_T = 1\ \mathrm{m}^3$) per unit head decline ($dh = -1\ \mathrm{m}$) due to rock compression:

$$V_{wr} = c_m \alpha_b \gamma_w \tag{29}$$

Also, the volume of water expansion due to water pressure decline is given by:

$$dV_{wp} = -c_w n V_T dp_f \tag{30}$$

where $c_w$is water compressibility at constant temperature and n is the effective porosity. Again, expressing fluid pressure in terms of water head $dp_f = \gamma_w\ dh$, the volume of water produced by a unit volume of rock $V_T = 1\ \mathrm{m}^3$ under a unit head decline $dh = -1\mathrm{m}$ due to water expansion is:

$$V_{wp} = c_w n \gamma_w \tag{31}$$

Finally, combining Eq (29) and Eq (31), we obtain the total volume of water produced per unit rock thickness and per unit head decline:

$$S_s = \gamma_w (\alpha_b c_m + n c_w) \tag{32}$$

where S_s is the specific storage. The compaction coefficient can be then expressed as:

$$c_m = \frac{1}{\alpha_b}\left(\frac{S_s}{\gamma_w} - c_w n\right) \tag{33}$$

4.2 Subsidence from hydrogeological parameters

Neglecting the effect of coal shrinkage on the storage characteristics of coal seams, changing pressures to hydrostatic heads and combining Eq (19) and Eq (33)) leads to:

$$\Delta h = S_s\ h\Delta H - n c_w h \Delta H + h \varepsilon_L \frac{K}{H_{us}}\left(\frac{H_f}{H_{L\varepsilon} + H_f} - \frac{H_{fi}}{H_{L\varepsilon} + H_{fi}}\right) \tag{34}$$

where H_f and $H_{f\mathrm{i}}$ are the current and initial hydrostatic heads, and $H_{L\varepsilon}$ is the Langmuir head equivalent to the Langmuir pressure for shrinkage strain ($p_{L\varepsilon}$). The terms on the right hand side of Eq (34) represent the mechanical compaction, fluid expansion and coal shrinkage processes, respectively.

It is noted that Δh in Eq (34) returns the total compaction in coal seams, which is not necessarily equal to the subsidence at the ground surface, depending on the competence of the overlying strata in hampering the transmission of a fraction of the compaction to the surface and also the compaction from the surrounding units.

5 Exploring the contribution of shrinkage to CSG-induced subsidence

5.1 Overall approach

In this chapter, the derived equation for subsidence (Eq (34) is used to understand the relative contribution of coal shrinkage in subsidence. Parameters are compiled using information available for the Surat CMA. The results from a representative parameter set are used to demonstrate the expected shrinkage contribution. Following this, an uncertainty analysis is carried out to describe the potential range of coal shrinkage in the study area, constrained by the local parameter ranges. A sensitivity analysis is subsequently undertaken to quantify the relative importance of different parameters in the subsidence calculation, given their prior probability distributions. The interburden units are also included in the analysis. It is assumed that an instantaneous head equilibrium can be obtained during CSG depressurisation and all the compaction to the subsurface units can be realised on the ground surface. Thus, the analysis in the section is a conservative assessment.

5.2 Parameter estimation

The hydrogeological parameters used in the subsequent analysis are based on OGIA's previous work in the Surat CMA (OGIA 2021) (Table 1). Specific storage of coal seams and interburden are based on a numerical groundwater model that is calibrated using InSAR data. The thicknesses of coal and interburden are based on statistics from well logs. A representative total thickness of 300 m was used for the Walloon Coal Measures and an initial head of 300 m was selected based on monitoring data from the study area.

Table 1: Hydrogeological parameters used for the parametric study

Parameter	Min	Mean	Max	Std
Ss_{coal} (log10)	-6.4	-5.5	-4.9	0.2
$Ss_{interburden}$ (log10)	-7.9	-6.9	-6.0	0.3
Coal proportion (log10)	-1.7	-1.0	-0.3	0.23

Table 2 presents some statistics of the Langmuir strain parameters for different units of the Walloon Coal Measures. These values are obtained using Eq (14), which relates Langmuir isotherm parameters for gas content to shrinkage strain. Seven methane adsorption reports (Queensland Government, Department of Resources, 2016) from the study area have subsequently been used to obtain estimates of Langmuir parameters V_L and P_L. A cross-plot of limited available ε_L and V_L data from other coal basins (Figure 7) yields a proportionality coefficient (β_h) of 1.06 kg/m^3 for Eq (14). The Langmuir pressure for sorptive strain ($P_{L\varepsilon}$) is assumed to be equal to P_L from methane adsorption tests, however it is noted that this is not always the case. Experimental analysis of local coal samples is required to directly obtain ε_L and $P_{L\varepsilon}$ values for the area of interest.

Table 2: Statistics of the volumetric shrinkage strain parameters for the study area

Coal measure	Property	Count	Min	Mean	Max	Std
Upper Juandah	Langmuir strain (micro strain)	47	2193	8871	14358	2922
	Langmuir head for shrinkage strain (m water)		151	461	1220	153
Lower Juandah	Langmuir strain (micro strain)	36	702	11865	16677	3993
	Langmuir head for shrinkage strain (m water)		377	577	1,657	273
Taroom	Langmuir strain (micro strain)	29	5109	12534	16518	2865
	Langmuir head for shrinkage strain (m water)		423	577	802	96

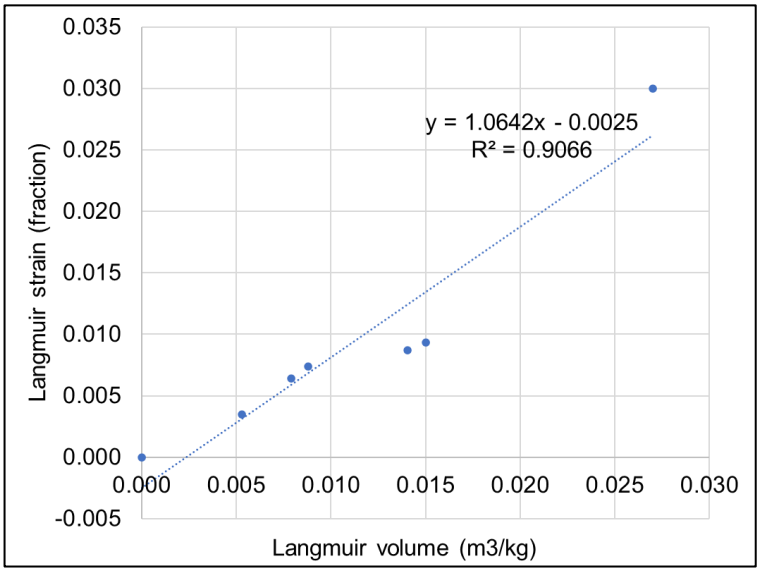

Figure 7: Langmuir strain (ε_L) versus Langmuir volume (V_L) based on limited available data from North American coal basins

5.3 Shrinkage estimation from a representative parameter set

This section presents generalised results, using the mean of the estimated parameter ranges in the previous section to provide qualitative and quantitative insights into the compaction and shrinkage processes in a coal seam.

Figure 8a shows the variation of poromechanical compaction, desorption-induced shrinkage and subsidence for hydrostatic head drops from 10 to 500 m. Consistent with their respective equations, poromechanical compaction and desorption-induced shrinkage increase with hydrostatic head drop in linear and non-linear manners, respectively. The non-linearity of coal shrinkage as a function of hydrostatic head implies that coal shrinkage for unit of pressure/head drop increases during the gas production life of a CSG well. The coal sample (cell in a numerical modelling context) will experience no further shrinkage after reaching its asymptote corresponding to their abandonment gas content.

Figure 8b shows the same results in a 100% stacked column plot, where it can be seen the proportion of coal shrinkage in the total compaction increases approximately from 58% to 77% as hydrostatic

head falls. This is consistent with the change in the slope of the shrinkage strain versus pore pressure curve. For a coal thickness of 30 m, an interburden thickness of 270 m and a hydrostatic head reduction of 500 m, the coal compaction, coal shrinkage and interburden compaction in the subsurface will be approximately 45, 190, and 20 mm, respectively. The total compaction of the coal seams will be approximately 255 mm in this case, which may or may not fully reach the ground surface as other factors such as the bridging effect of competent strata can hinder the collective settlement of overlying formations (Lowe 2012).

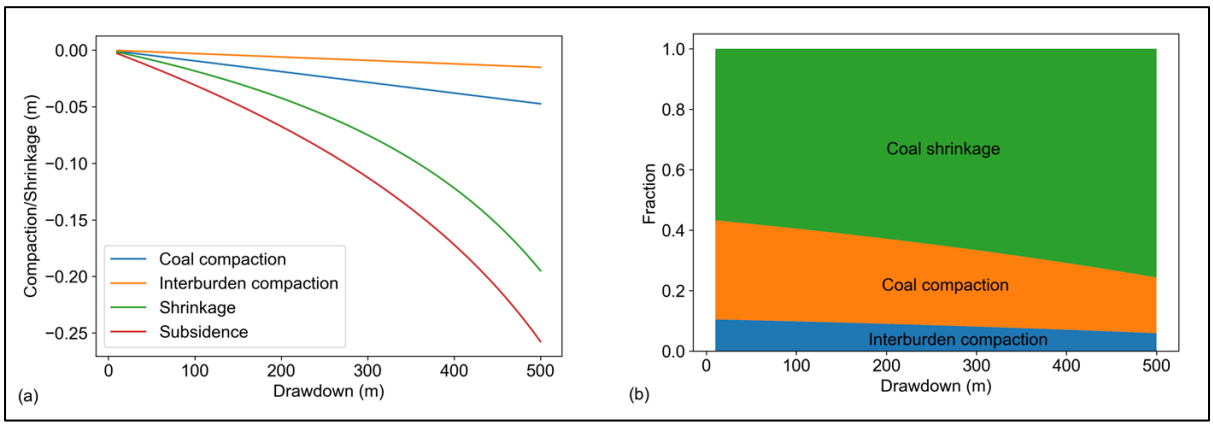

Figure 8: Poromechanical compaction and desorption-induced shrinkage for different cases of hydrostatic drop

5.4 Estimating predictive variability

Further to the above, Monte Carlo uncertainty analysis was conducted on the prior parameter distributions to understand the potential contribution of coal shrinkage to subsidence. Specific storage and coal proportion parameters are assumed to follow log-normal distribution, while normal distributions are used for other parameters in Eq (20) and Eq (34). Correlations between parameters are ignored in the analysis. A total of 10,000 parameter samples were drawn from the aforementioned distributions.

As the drawdown increases from 20 to 500 m during CSG depressurisation, the expected shrinkage fraction grows from 0.65 to 0.8 (Figure 10). The growing of shrinkage in Eq (34) is not linear as more drawdown is realised, resulting in a higher shrinkage fraction at the later stages of CSG depressurisation. If the interburden compaction is not included in the analysis, the expected (p50) shrinkage fraction varies between 0.54 and 0.73 for the same range in drawdown (Figure 10)

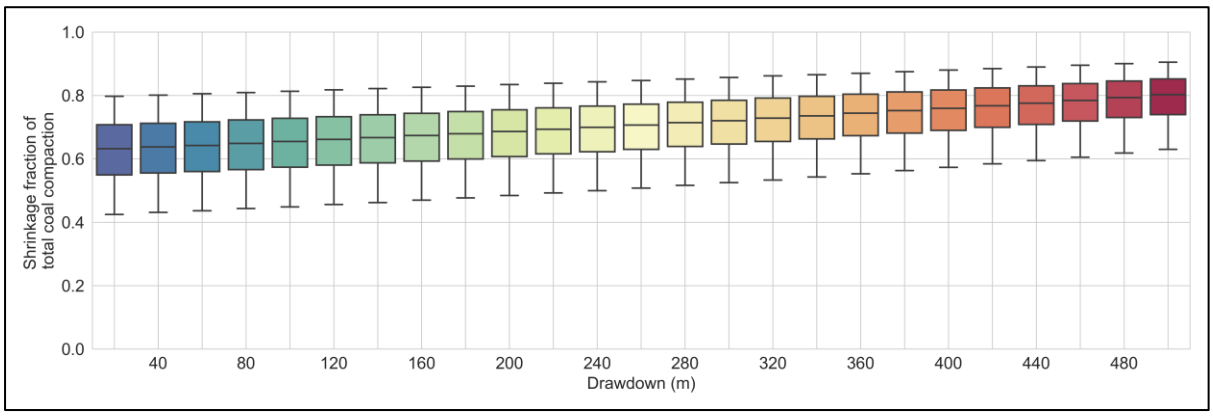

Figure 9: Coal shrinkage fraction of total coal compaction as a function of drawdown

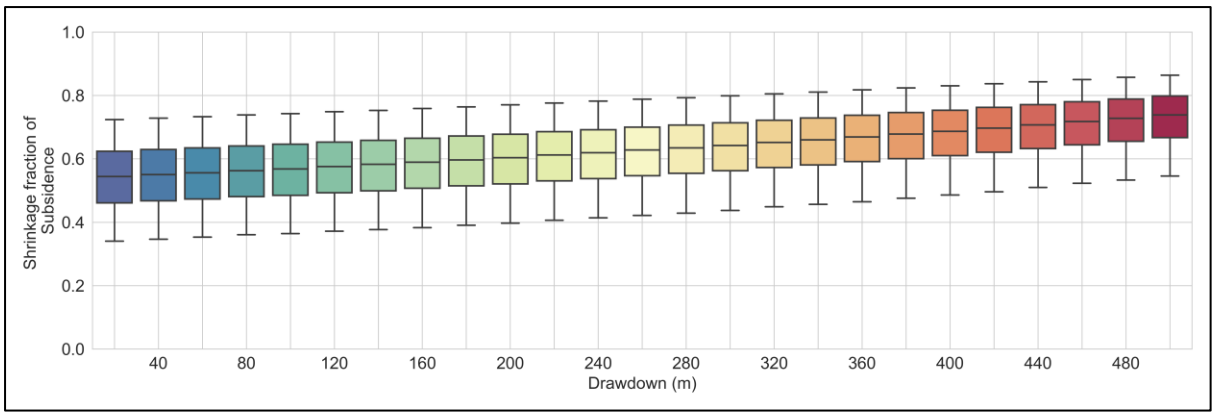

Figure 10: Coal shrinkage fraction of subsidence as a function of drawdown

The potential shrinkage fraction of subsidence generally follows a normal distribution for a specific drawdown (Figure 11). For a particular drawdown, the shrinkage fraction shows a high uncertainty. For example, for 500 m of drawdown, it can vary from 0.1 to 0.9 with a mean of around 0.73. This can be attributed to the high sensitivity of subsidence to controlling parameters and also the wide prior ranges of parameters.

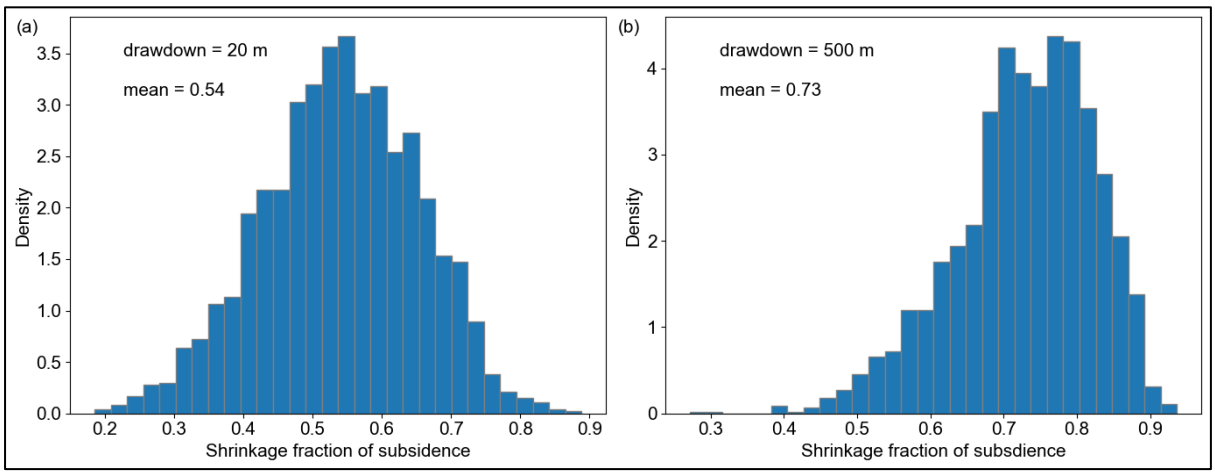

Figure 11: Distribution of shrinkage fraction for drawdown of a) 20 m and b) 500 m

The maximum specific storage for coal used in the current analysis is 1.25E-5 m^{-1}. If this is increased to 5.00E-5 m^{-1}, the relative roles of shrinkage will change significantly, particularly in the early stage of the depressurisation. This further demonstrates the importance of constraining parameter ranges for specific storage and for Langmuir strain in the current formulation of subsidence (Figure 12).

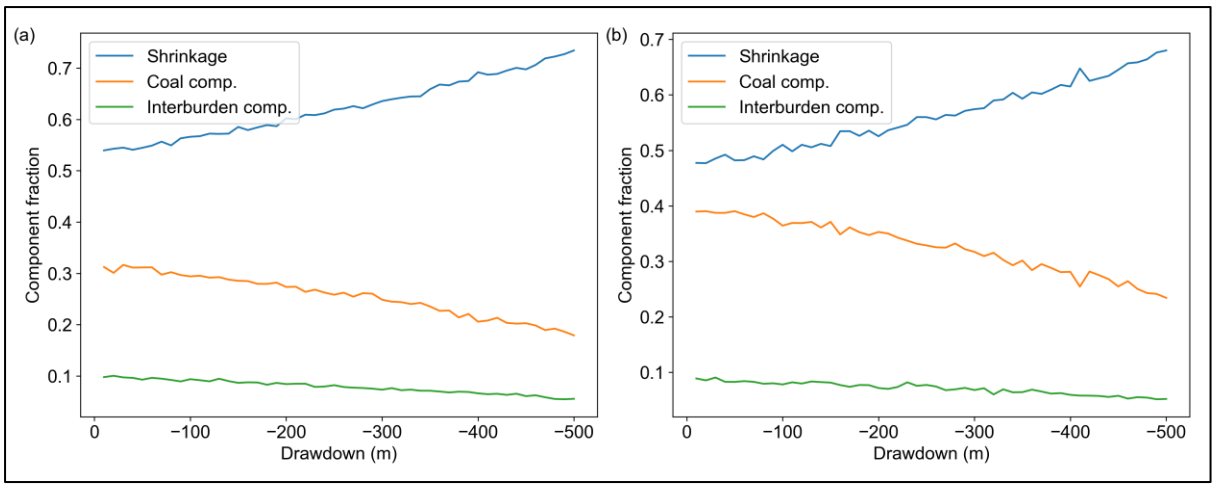

Figure 12: P50 relative contribution of different processes to subsidence as the increase of drawdown, using maximum Ss of 1.25E-5 m^{-1} (a) and 5.00E-5 m^{-1} (b)

5.5 Investigating parameter contributions to predictive variability

A traditional sensitivity analysis was conducted to explore the variability of coal shrinkage proportion based on the prior probability distributions for key parameters (outlined in Table 1 and Table 2). The parameters assessed included coal specific storage, interburden specific storage, coal proportion, Langmuir strain, Langmuir head.

The analysis varied parameters one at a time by drawing 10,000 samples from the prior while fixing the value for all other parameters at the mean. Figure 13 shows the range of shrinkage proportions above and below the mean for each parameter. Based on the analysis, coal specific storage is the most sensitive parameter with respect to coal shrinkage proportion. The two other parameters to which the coal shrinkage proportion is also highly sensitive are the Langmuir strain (which controls the magnitude of shrinkage) and the interburden specific storage – given its large proportion (on average 90%) of coal measures. The next most sensitive parameters are coal proportion and Langmuir head.

Overall, subsidence estimation is considered sensitive to all five parameters. This highlights the significance of obtaining a good measurement/estimate of these parameters. It also demonstrates the need for calibration-constrained uncertainty analysis to effectively reduce uncertainty by constraining parameter ranges and to effectively explore coal shrinkage and subsidence for predictive models.

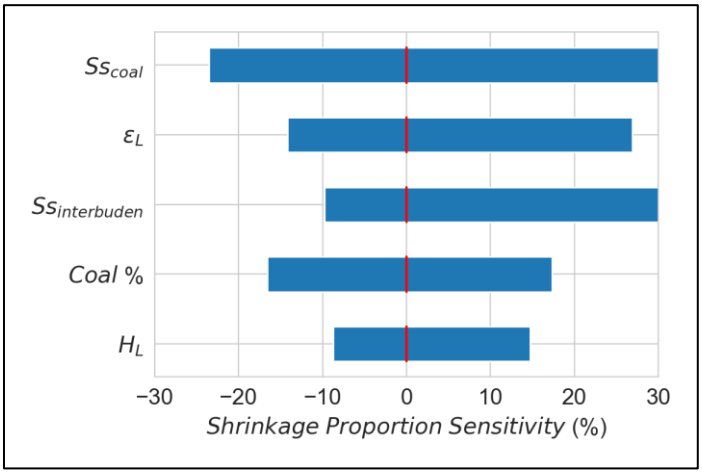

Figure 13: Traditional sensitivity analysis for shrinkage proportion based on prior parameter distributions for five key parameters.

6 Discussion

Coal shrinkage is a process that may contribute to the total CSG-induced subsidence realised at the ground surface. The amount of coal shrinkage in a given time period is proportional to the corresponding change in gas content. It also depends on coal properties, such as Langmuir isotherm and shrinkage strain parameters, which vary by coal composition and rank. Past research has extensively addressed the effect of coal matrix shrinkage on coal permeability evolution – through analysing measurements at both laboratory and field scales – as well as developing analytical and numerical models. The effect of coal shrinkage on subsidence in CSG fields, however, has been relatively unexplored until recently, when researchers from the University of Queensland highlighted its importance.

OGIA's data-driven approach to subsidence modelling has so far implicitly represented coal shrinkage because of history-matching to regional observations of ground motion. To better represent the process and improve predictive capability in future modelling, however, OGIA has been exploring this further through an analytical subsidence model derived in the current study, particularly to integrate poromechanical compaction due to pressure drop and shrinkage as a result of gas desorption from the coal matrix. The shrinkage component is based on Langmuir-type relations between gas content and pore fluid pressure. It lends itself well to coupling with numerical groundwater models through shared variables including specific storage and pressure/head.

A prior Monte Carlo uncertainty analysis was conducted by randomly sampling the parameter space 10,000 times. Given the currently identified parameter ranges, the uncertainty analysis suggests that the expected shrinkage fraction of the total subsidence – neglecting other contributing factors such as the shielding effect – grows from ~0.54 to 0.73 as the drawdown increases from 20 to 500 m during CSG depressurisation. This result indicates that coal shrinkage is likely to play a significant role in the total subsidence realised at the surface.

A sensitivity analysis of key parameters shows that the coal shrinkage estimation is most sensitive to the specific storage of coal. The Langmuir strain and the specific storage of interburden are the two other parameters to which the estimation of coal shrinkage is sensitive to a relatively large extent.

The large range in predictive variability from the uncertainty analysis highlights the significance of obtaining a good measurement/estimate of these parameters. It also demonstrates the need for calibration-constrained uncertainty analysis to appropriately explore coal shrinkage and subsidence for predictive models. Limited experimental data are currently available on coal shrinkage properties in the Surat CMA and as such, OGIA is currently exploring options to obtain measurements of Langmuir strain and pressure from core data in the Surat CMA to better constrain shrinkage models.

OGIA's coal compaction model does not account for inelasticity or the gas diffusion process. Inelasticity can potentially affect subsidence where large drawdowns take place. Ignoring the effect of the diffusion process likely leads to an overestimation of the shrinkage rate, even though the estimate of total shrinkage corresponding to the abandonment gas content is within an acceptable interval. OGIA is also evaluating methods to represent the diffusion process in modelling coal shrinkage.

7 Where to from here

The work presented in this document lays the foundation for a larger project to develop rapid, stochastic and local-scale numerical models to predict subsidence impacts from CSG developments. The subsidence model presented in this document will be coupled with 3D transient numerical groundwater models to assess the transient evolution of subsidence in the Surat CMA during CSG depressurisation.

These models will draw heavily on a large dataset of subsidence observations derived from the latest InSAR technology, which is currently the data most pertinent to subsidence and which shows significant promise for constraining key parameters for groundwater flow modelling, such as specific storage. The overarching methodology applied in these models will rely on a hybrid data/process-driven approach and so, while the relevant processes such as coal shrinkage will be represented, they must also be simplified as outlined in this document – decreasing computation overheads for model run times and allowing for a comprehensive and stochastic calibration to InSAR data. It is envisaged that these models will be coupled with state-of-the-art signal separation models to absorb non-CSG signals as well as noise in observations and to facilitate increased fits to subsidence observations.

Ultimately, these models will be designed to reduce the uncertainty of future subsidence impact predictions and it is hoped they will be able to inform impact assessments and the development of subsidence managemnent strategies.

8 Conclusions

- CSG-induced subsidence at the surface is likely to be driven by coal shrinkage as well as by poromechanical compaction.
- Based on the presented analytical model and its underlying assumptions, coal shrinkage is likely to be the dominant process in the context of the Surat Basin.
- Although OGIA's data-driven approach to regional subsidence modelling has so far implicitly represented coal shrinkage through calibration to InSAR (which is considered fit for purpose), a more refined approach will be necessary to explicitly accommodate the process in future farm-scale assessments.
- The amount of coal shrinkage in a given time period is proportional to the corresponding change in gas content. It also depends on coal properties, such as Langmuir isotherm and shrinkage strain parameters, which vary by coal composition and rank.
- Langmuir strain is a key parameter in constraining the modelled proportion of coal shrinkage in subsidence. OGIA is therefore planning to collect additional laboratory measurements of this parameter in the Surat Basin.
- Future subsidence models by OGIA will incorporate the shrinkage formulation described in this document and will aim to assimilate the available data on shrinkage parameters and calibration to ground motion data.

9 References

Aghighi, MA, Lv, A & Roshan, H 2021, 'Non-equilibrium thermodynamics approach to mass transport in sorptive dual continuum porous media: A theoretical foundation and numerical simulation', *Journal of Natural Gas Science and Engineering*, vol. 87.

Aghighi, MA, Lv, A, Siddiqui, MAQ, Masoumi, H, Thomas, R & Roshan, H 2022, 'A Multiphysics Field-Scale Investigation of Gas Pre-Drainage in Sorptive Sediments', *International Journal of Coal Geology*, vol. 261.

Bear, J & Corapcioglu, MY 1981, 'A mathematical model for consolidation in a thermoelastic aquifer due to hot water injection or pumping', *Water Resources Research*, vol. 17, no. 3, pp. 723–736.

Bottomley, W, Furniss, JP, Raza, SS, Ge, L & Rudolph, V 2017, 'Characterising the dependence of coal permeability to methane adsorption, pore pressure and stress: Laboratory testing of Walloon Coals from the Surat Basin', in *SPE/IATMI Asia Pacific Oil & Gas Conference and Exhibition*, OnePetro.

Burgoyne, M & Shrivastava, R 2016, 'A practical workflow for characterizing stress-dependent behaviour of coal from changes in well productivity', *Journal of Natural Gas Science and Engineering*, vol. 33, pp. 1025–1045.

Cai, Y, Liu, D, Mathews, JP, Pan, Z, Elsworth, D, Yao, Y, Li, J & Guo, X 2014, 'Permeability evolution in fractured coal—Combining triaxial confinement with X-ray computed tomography, acoustic emission and ultrasonic techniques', *International Journal of Coal Geology*, vol. 122, pp. 91–104.

Chen, Z, Liu, J, Elsworth, D, Pan, Z & Wang, S 2013, 'Roles of coal heterogeneity on evolution of coal permeability under unconstrained boundary conditions', *Journal of Natural Gas Science and Engineering*, vol. 15, pp. 38–52.

Commonwealth of Australia 2014, *Monitoring and management of subsidence induced by coal seam gas extraction*, Canberra, accessed March 21, 2019, from <www.iesc.environment.gov.au>.

Cui, X & Bustin, RM 2005, 'Volumetric strain associated with methane desorption and its impact on coalbed gas production from deep coal seams', *AAPG Bulletin*, vol. 89, no. 9, pp. 1181–1202.

Dudley, JW, Brignoli, M, Crawford, BR, Ewy, RT, Love, DK, McLennan, JD, Ramos, GG, Shafer, JL, Sharf-Aldin, MH & Siebrits, E 2016, 'ISRM suggested method for uniaxial-strain compressibility testing for reservoir geomechanics', *Rock Mechanics and Rock Engineering*, vol. 49, pp. 4153–4178.

Durucan, S, Ahsanb, M & Shia, J-Q 2009, 'Matrix shrinkage and swelling characteristics of European coals', *Energy Procedia*, vol. 1, no. 1, pp. 3055–3062.

Erling Fjær, Rune Holt, Per Horsrud, AR 2008, *Petroleum Related Rock Mechanics* 2nd edn,.

Espinoza, DN, Vandamme, M, Dangla, P, Pereira, J-M & Vidal-Gilbert, S 2013, 'A transverse isotropic model for microporous solids: Application to coal matrix adsorption and swelling', *Journal of Geophysical Research: Solid Earth*, vol. 118, no. 12, pp. 6113–6123, accessed from <https://doi.org/10.1002/2013JB010337>.

Freeze, RA & Cherry, JA 1979, *Groundwater*, Prentice-Hall, Englewood Cliffs, NJ.

Galloway, DL & Burbey, TJ 2011, 'Review: Regional land subsidence accompanying groundwater extraction', *Hydrogeology Journal*, vol. 19, no. 8, pp. 1459–1486.

Geertsma, J 1973, 'Land Subsidence Above Compacting Oil and Gas Reservoirs', *Journal of Petroleum Technology*, vol. 25, no. 6, pp. 734–744.

Gray, I 1987, 'Reservoir Engineering in Coal Seams: Part 2-Observations of Gas Movement in Coal Seams', *SPE Reservoir Engineering*, vol. 2, no. 01, pp. 35–40.

Hanson, RT, Anderson, SR & Pool, DR 1990, *Simulation of ground-water flow and potential land subsidence, Avra Valley, Arizona*, US Department of the Interior, US Geological Survey.

Harpalani, S & Chen, G 1992, 'Effect of gas production on porosity and permeability of coal', in *Proceedings of the Symposium of Coalbed Methane R and D in Australia*, pp. 67–73.

Harpalani, S & Schraufnagel, RA 1990, 'Shrinkage of coal matrix with release of gas and its impact on permeability of coal', *Fuel*, vol. 69, no. 5, pp. 551–556.

Holzer, TL & Galloway, DL 2005, 'Impacts of land subsidence caused by withdrawal of underground fluids in the United States',.

Hummel, N, Rai, UB, Dudley, JW, Schutjens, P, Gear, I, Sutton, H & McKelvey, P 2021, 'Unlocking Methane Desorption Effects in Reservoir Compaction and Subsidence Computations for a Coal Seam Gas Development', in *82nd EAGE Annual Conference & Exhibition*, EAGE Publications BV, pp. 1–5.

Jaeger, JC, Cook, N & Zimmerman, R 2007, 'Fundamentals of Rock Mechanics, 4th Edition, Wiley-Blackwell, May 2007, 488 pages, Hardcover, ISBN: 978-0-632-05759-7, US 88.00.', *Wiley*, vol. 470, no. 3–4, p. 345.

Jayeoba, A 2020, 'Numerical simulation of ground surface subsidence due to coal-bed methane extraction',.

Karthikeyan, G, Chand, J & Chatterjee, R 2020, 'Impact of geomechanics in coal bed methane development and production, Barakar coals in central India', *Journal of Petroleum Science and Engineering*, vol. 194, p. 107515.

Khan, SD, Huang, Z & Karacay, A 2014, 'Study of ground subsidence in northwest Harris county using GPS, LiDAR, and InSAR techniques', *Natural Hazards*, vol. 73, pp. 1143–1173.

Levine, JR 1996, 'Model study of the influence of matrix shrinkage on absolute permeability of coal bed reservoirs', *Geological Society, London, Special Publications*, vol. 109, no. 1, p. 197.

Liu, A, Liu, S, Liu, P & Harpalani, S 2021, 'The role of sorption-induced coal matrix shrinkage on permeability and stress evolutions under replicated in situ condition for CBM reservoirs', *Fuel*, vol. 294, p. 120530.

Liu, J, Ma, T, Fu, J, Fan, X & Zhang, Q 2022, 'Fully coupled thermo-hydro-mechanical model for wellbore stability analysis of a CBM horizontal well', in *56th US Rock Mechanics/Geomechanics Symposium*, OnePetro.

Liu, T, Zhao, Y, Kong, X, Lin, B & Zou, Q 2022, 'Dynamics of coalbed methane emission from coal cores under various stress paths and its application in gas extraction in mining-disturbed coal seam', *Journal of Natural Gas Science and Engineering*, vol. 104, p. 104677.

Lowe, M 2012, *Subsidence in sedimentary basins due to groundwater withdrawal for geothermal energy development*, Utah Geological Survey.

Lv, A, Aghighi, MA, Masoumi, H & Roshan, H 2021, 'On swelling stress–strain of coal and their interaction with external stress', *Fuel*, p. 122534.

Lv, A, Cheng, L, Aghighi, MA, Masoumi, H & Roshan, H 2021, 'A novel workflow based on physics-informed machine learning to determine the permeability profile of fractured coal seams using downhole geophysical logs', *Marine and Petroleum Geology*, vol. 131, p. 105171.

Masoudian, M., Leonardi, C, Chen, Z & Underschultz, J 2019, 'The effect of sorption-induced shrinkage on the ground surface movement above gas-producing coalbeds',.

Meredith, E, Kuzara, S, Wheaton, J, Bierbach, S & Don, S 2015, *2014 Annual Coalbed-Methane Regional Groundwater Monitoring Report: Powder River Basin, Montana*, Montana Bureau of Mines and Geology.

Morton, R, Bernier, J & Barras, J 2006, 'Evidence of regional subsidence and associated interior wetland loss induced by hydrocarbon production, Gulf Coast region, USA', *Environmental Geology*, vol. 50, no. 2, pp. 261–274.

Nagel, NB 2001, 'Compaction and subsidence issues within the petroleum industry: From Wilmington to Ekofisk and beyond', *Physics and Chemistry of the Earth, Part A: Solid Earth and Geodesy*, vol. 26, no. 1–2, pp. 3–14.

Naraj, NO 2020, 'Monitoring the Earth's surface subsidence phenomena in mining areas',.

OGIA 2021, *Underground Water Impact Report 2021 for the Surat Cumulative Management Area*, Brisbane, Australia, accessed from <https://www.rdmw.qld.gov.au/__data/assets/pdf_file/0008/1584728/uwir-2021-report.pdf>.

Palmer, I & Mansoori, J 1996, 'How permeability depends on stress and pore pressure in coalbeds: a new model', in *SPE Annual Technical Conference and Exhibition*, Society of Petroleum Engineers.

Palmer, I & Mansoori, J 1998, 'How Permeability Depends on Stress and Pore Pressure in Coalbeds: A New Model', *Spe Reservoir Evaluation & Engineering*, vol. 1, no. 06, pp. 539–544.

Pan, Z & Connell, LD 2012, 'Modelling permeability for coal reservoirs: A review of analytical models and testing data', *International Journal of Coal Geology*, vol. 92, pp. 1–44, accessed May 16, 2019, from <https://www.sciencedirect.com/science/article/abs/pii/S0166516211002722>.

Poland, JF & Davis, GH 1969, 'Land subsidence due to withdrawal of fluids',.

Raza, SS, Rudolph, V, Rufford, T & Chen, Z 2020, 'A Stochastic Method to Estimate the Anisotropic Stress-Dependent Coal Permeability by Pore-Volume Distribution and Stress-Strain Measurements', *Spe Journal*.

Reisabadi, MZ, Haghighi, M, Sayyafzadeh, M & Khaksar, A 2020, 'Effect of matrix shrinkage on wellbore stresses in coal seam gas: An example from Bowen Basin, east Australia', *Journal of Natural Gas Science and Engineering*, vol. 77, p. 103280.

Robertson, EP 2005, 'Measurement and Modeling of Sorption-Induced Strain and Permeability Changes in Coal', *Idaho National Lab.(INL), Idaho Falls, ID (United States)*, no. INL/EXT-06-11832.

Robertson, EP & Christiansen, RL 2006, 'A Permeability Model for Coal and Other Fractured, Sorptive-Elastic Media', *SPE Eastern Regional Meeting*, p. 12.

Salmachi, A, Rajabi, M, Wainman, C, Mackie, S, McCabe, P, Camac, B & Clarkson, C 2021, 'History, geology, in situ stress pattern, gas content and permeability of coal seam gas basins in Australia: A review', *Energies*, vol. 14, no. 9, p. 2651.

Shi, JQ & Durucan, S 2004, 'Drawdown Induced Changes in Permeability of Coalbeds: A New Interpretation of the Reservoir Response to Primary Recovery', *Transport in Porous Media*, vol. 56, no. 1, pp. 1–16.

Teatini, P, Ferronato, M, Gambolati, G & Gonella, M 2006, 'Groundwater pumping and land subsidence in the Emilia-Romagna coastland, Italy: Modeling the past occurrence and the future trend', *Water Resources Research*, vol. 42, no. 1.

Wei, Z & Zhang, D 2010, 'Coupled fluid-flow and geomechanics for triple-porosity/dual-permeability modeling of coalbed methane recovery', *International Journal of Rock Mechanics and Mining Sciences*, vol. 47, no. 8, pp. 1242–1253.

Wu, Y, Liu, J, Elsworth, D, Chen, Z, Connell, L & Pan, Z 2010, 'Dual poroelastic response of a coal seam to CO2 injection', *International Journal of Greenhouse Gas Control*, vol. 4, no. 4, pp. 668–678.

Yang, J & Luo, Y 2021, 'Enhanced subsurface subsidence prediction model incorporating key strata theory', *Mining, Metallurgy & Exploration*, vol. 38, no. 2, pp. 995–1008.

Zhong, R, Leonardi, CR, Mitchell, TR & Johnson Jr, RL 2021, 'Wellbore stability analysis of horizontal drilling in Bowen and Surat coal seam gas wells', in *Asia Pacific Unconventional Resources Technology Conference, Virtual, 16–18 November 2021*, Unconventional Resources Technology Conference (URTeC), pp. 552–567.

Zoback, MD 2010, *Reservoir geomechanics*, Cambridge University Press.

This page is intentionally blank.

Department of Regional Development,
Manufacturing and Water
GPO Box 2771, Brisbane, Queensland 4001
13 QGOV (13 74 68)
info@rdmw.qld.gov.au
rdmw.qld.gov.au

Queensland Government